In addition it is necessary to ensure the zero divergence of **B**. The latter follows directly from (17):

$$\nabla \cdot \mu(\mathbf{T} + \mathbf{K}i - \nabla\Omega) = 0 \qquad (19)$$

To use the finite element method, the formulation **T**-Ω must be converted into the equivalent weak formulation [**8**]**.** The vector potential **T** and the vector field **K** are discretized on the edges of the finite element mesh using the Whitney complex [**8**]. The scalar potential Ω is defined at the nodes of the mesh.

It should be noted that the formulation in the continuous domain does not guarantee a unique solution but uniqueness is guaranteed in the discrete, finite element domain. Since we need to find $\nabla \times \mathbf{T}$ and $\nabla\Omega$, the actual values of **T** and Ω are of no interest.

3. Non-linear model

As indicated above, the model is non-linear due to the semiconducting layer. The measurements are carried out across the semiconductor layer. A voltage is imposed across the two conductors and the current through the semiconducting layer is measured. **Figure 6** shows the electrical field **E** in the sheet based on the current density through the sheet.

To model the semiconductor we use a simple regression. The relationship between E and J is $E = aJ^b$ with a and b respectively equal 6081 and 0.301. These values were extracted from the experimental measurements since no data on the nonlinear behavior of metal oxide junctions could be found. Obviously, other junctions will characteristics and these need to be established.

The solver used to obtain the non-linear solution is the fixed-point method.

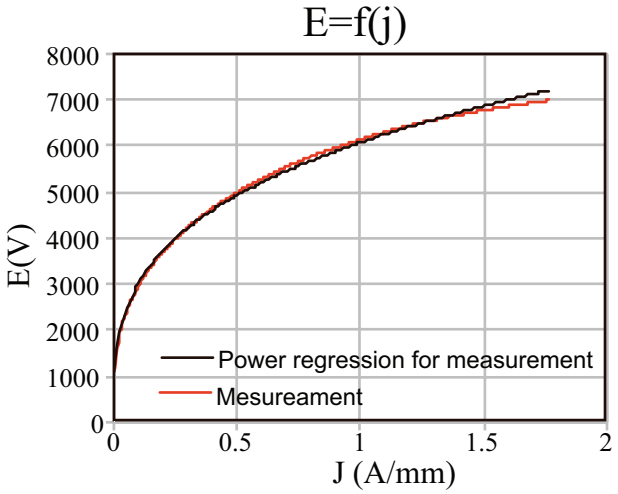

Figure 6: Electrical field as a function of current density in the semiconducting layer.

4. Results

The nonlinear model above was applied to a simple geometry that duplicates the experimental configuration in **Fig. 4a** with $i = 5 \times 10^{-3} \sin(\omega t)$ the current imposed through the model and **K** a vector field such that $\nabla \times \mathbf{K} = \hat{\mathbf{y}}$. The model is shown in **Fig. 7** and is made of two steel disks and a semiconducting layer (black) sandwiched between them. The figure shows as well the finite element mesh (only the elements on the outer surface are visible). The current distribution in the middle of the model is shown in **Fig. 8**. The skin depth in steel is clearly visible. **Fig. 9** is the terminal voltage showing the nonlinear effect of the semiconducting layer. This waveform has been previously observed in work on the rusty bolt effect [7]

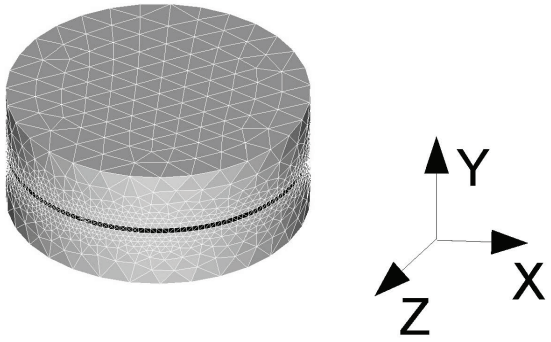

Figure 7: The model used for computation. The finite element mesh can be seen on the surface. The iron oxide layer is sandwiched between two steel disks.

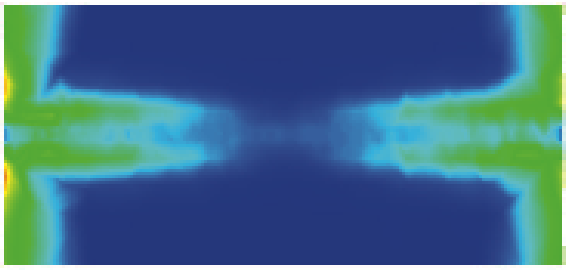

Figure 8: Current distribution in the model.

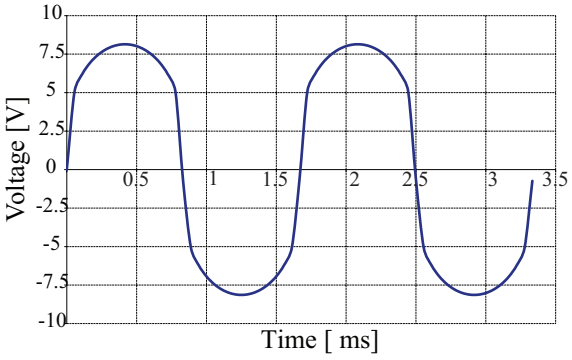

Figure 9: Evolution in time of the terminal voltage.

5. Conclusions

A simple nonlinear model based on the formulation of Maxwell's equations in terms of the electric vector potential T and magnetic scalar potential W with nonlinear conductivity has been presented for the purpose of modeling corrosion. The nonlinearity is derived from experimental data. The results show the expected characteristics of clipped sinusoidal voltage that has been observed in work on the rusty bolt effect. The current model is expected to provide a means of more accurate modeling of the effects observed in corrosion in pipes and other structure by the introduction of the rectification effects.

References

1. H. Gräfen, E.M. Horn, H. Schlecker and H. Schindler, H. "*Ullmann's Encyclopedia of Industrial Chemistry*," Wiley, 2000.
2. S. Goidanich, L. Lazzari and M. Ormellese "AC corrosion. Part 2: Parameters influencing corrosion rate," *Corrosion Science*, Vol. 52, 916–922, 1986.
3. R Zhang, P.R. Vairavanathan and S.B. Lalvani, "Perturbation method analysis of AC induced corrosion," *Corrosion Science*, Vol. 50, 1664-1671, 2008.
4. N. Ida, J. H. Payer, and X. Shan, "Electromagnetic Radiation Effects on Corrosion," in Proceedings of the DoD Corrosion Conference, July 31 – August 5, 2011.
5. J. H. Payer, N. Ida, and X. Shan "AC-Induced Corrosion and Interactions with Cathodic Protection," in Proceedings of the DoD Corrosion Conference, July 31 – August 5, 2011.
6. I. Ibrahim, M. Meyer, B. Tribolet, H. Takenouti, S. Joiret, S. Fontaine and H.G. Schoneich, "On the mechanism of AC assisted corrosion of buried pipelines and its CP mitigation," Proc. IPC, 1-25, 2008.
7. R. Haynes, H.W. Carhart and J.C. Cooper, "Chemical reduction of intermodulation interference caused by metal-oxide-metal junctions aboard ships," Naval Research Laboratory report AD-A239 530, July 31, 1991.
8. A.Bossavit, "Electromagnétisme en vue de la modélisation", édition Springer-Verlag, 1993.